



HAL
open science

LHR band emissions at mid-latitude and their relationship to ionospheric ELF hiss and relativistic electrons

A. Morioka, H. Oya, T. Obara, Y. S. Miyoshi, K. Nagata, K.-I. Oyama, T. Abe

► **To cite this version:**

A. Morioka, H. Oya, T. Obara, Y. S. Miyoshi, K. Nagata, et al.. LHR band emissions at mid-latitude and their relationship to ionospheric ELF hiss and relativistic electrons. *Annales Geophysicae*, 2005, 23 (3), pp.723-732. <hal-00317602>

HAL Id: hal-00317602

<https://hal.science/hal-00317602v1>

Submitted on 18 Jun 2008

HAL is a multi-disciplinary open access archive for the deposit and dissemination of scientific research documents, whether they are published or not. The documents may come from teaching and research institutions in France or abroad, or from public or private research centers.

L'archive ouverte pluridisciplinaire **HAL**, est destinée au dépôt et à la diffusion de documents scientifiques de niveau recherche, publiés ou non, émanant des établissements d'enseignement et de recherche français ou étrangers, des laboratoires publics ou privés.



HAL Authorization

LHR band emissions at mid-latitude and their relationship to ionospheric ELF hiss and relativistic electrons

A. Morioka¹, H. Oya², T. Obara³, Y. S. Miyoshi⁴, K. Nagata⁵, K.-I. Oyama⁶, and T. Abe⁶

¹Planetary Plasma and Atmospheric Research Center, Tohoku University, Aoba-ku, Sendai, 980–8578, Japan

²Fukui University of Technology, 3-6-1, Gakuen, Fukui, 910-8505, Japan

³National Institute of Information and Communications Technology, 4-2-1, Nukiikitamachi, Koganei, 184-8795, Japan

⁴Solar-Terrestrial Environment Laboratory, Nagoya University, Honohara, Toyokawa, 422-8507, Japan

⁵Faculty of Engineering, Tamagawa University, 6-1-1, Tamagawagakuen, Machida, Tokyo, 194-8610, Japan

⁶Institute of Space and Astronautical Science, Japan Aerospace Exploration Agency, Sagami-hara, 229-8510, Japan

Received: 15 September 2004 – Revised: 31 December 2004 – Accepted: 10 January 2005 – Published: 30 March 2005

Abstract. LHR band emissions observed at mid-latitude were investigated using data from the EXOS-C (Ohzora) satellite. A typical feature of the LHR band emissions is a continuous banded structure without burst-like and cut-off features whose center frequency decreases as the satellite moves to higher latitudes. A statistical analysis of the occurrence characteristics of the phenomena showed that mid-latitude LHR emissions are distributed inside the plasma-pause during magnetically quiet periods, and the poleward boundary of the emission region moves to lower latitudes as the magnetic activity increases. The altitude distribution of the waves suggests that the propagation in the LHR duct formed horizontally in the mid-latitude upper-ionosphere. The emission is closely related to the occurrence of ionospheric ELF hiss. It is also shown that LHR emissions are commonly observed in the slot region of the radiation belt, and they sometimes accompany the enhancement of the ionospheric electron temperature. The generation of the LHR band emissions is discussed based on the observed characteristics.

Keywords. Ionosphere (Mid-latitude ionosphere, Wave propagation, Wave-particle interaction)

1 Introduction

The history of the study of ionospheric LHR band emissions started with early scientific satellite observations. In 1963, the Canadian satellite Alouette 1 discovered VLF noise bands enhanced in the electric field component (Barrington and Belrose, 1963). These VLF phenomena had never been observed on the ground. Just after the discovery, the wave phenomena were tentatively named the Alouette hiss band.

The wave phenomena were soon presumed to be lower hybrid resonance (LHR) emissions in the ionosphere (Brice and Smith, 1964, 1965). This hypothesis was further supported by Barrington et al. (1965). In this paper, we use the term “LHR band emissions” for the present phenomena, although some other terms, such as LHR emissions and LHR noise band, were used in early studies on the phenomena. Some statistical features of the LHR band emissions were studied by McEwen and Barrington (1967) using the Alouette data. They reported two different types of LHR band emissions, polar and mid-latitude emissions, and found that the mid-latitude LHR band emissions have a maximum occurrence at an invariant latitude of about 55° . The frequency of the mid-latitude LHR band emissions varies systematically with respect to the satellite latitude, (Barrington et al., 1963). The latitudinal frequency variation of the LHR band emissions was also investigated in relation to magnetic disturbances (Boskova et al., 1983).

After the discovery of the LHR band emissions, numerous observations of the phenomena were carried out with various satellites, and the fundamental characteristics and origin of the banded emission were discussed (Smith et al., 1966; Taylor et al., 1969; Anderson and Gurnett, 1969; Laaspere et al., 1969; Laaspere and Taylor, 1970; Laaspere et al., 1971; Burtis, 1973; Ondoh and Murakami, 1975; Boskova et al., 1983; Nishino and Tanaka, 1987; Boskova et al., 1992; Chum et al., 2002). In these studies, the observed LHR frequency was confirmed to coincide with the calculated LHR frequency from an in-situ ion composition observation (Laaspere et al., 1969; Laaspere and Taylor, 1970). However, it is also reported that the observed LHR band frequency could not always be determined in the immediate vicinity of the spacecraft (Laaspere and Taylor, 1970). The magnetospheric LHR waves and related source characteristics above $\sim 1 R_E$ (R_E : Earth radii) have been reported by many satellite observations (e.g. Bell et al., 1994; Mikhailov et al., 1995; Jiříček et al., 2001, Tjulin et al., 2003).

Correspondence to: A. Morioka
(morioka@pparc.geophys.tohoku.ac.jp)

The source mechanism of the ionospheric LHR band emissions, which never propagate down to the ground and exhibit a characteristic frequency band nearly associated with the local LHR frequency, has not been clarified yet. Some arguments can be found from the standpoint of whistler-mode wave propagation in the ionosphere. Storey and Cerisier (1968) claimed that non-ducted whistler-mode waves propagating from the source enhance their electric field at the local LHR frequency in the ionosphere. On the other hand, Smith et al. (1966) proposed that the observed noise bands are the trapped waves in the ionospheric LHR duct. Gross (1970) extended this work and theoretically showed that an ionospheric duct oriented along a horizontal direction can be formed with a narrow wave guide. They claimed that the propagating auroral hiss through the ionospheric duct is the origin of the mid-latitude LHR emissions (Smith et al., 1966; Gross, 1970). As for the excitation process of the LHR band emissions, Horita and Watanabe (1969) proposed that a Landau instability caused by an electron stream of a few tens keV can excite continuous LHR band emissions with lower cut-off LHR frequencies. McBride and Pytte (1970) discussed this process in more detail by considering the collision effect on the electrostatic waves. They showed that the cut-off frequency changes with respect to the thermal spread of the electron stream.

Although the LHR band emissions in the ionosphere have been extensively studied since the discovery, the wave generation process and formation process of the banded LHR spectra in the upper ionosphere is not conclusive. The reason may lie partly in that the characteristics of the phenomena to establish the wave generation mechanism have not been sufficiently obtained. In this paper, we present some new characteristics of the LHR band emissions using a VLF data obtained by the EXOS-C (Ohzora), and discuss the possible generation mechanism of the emission.

2 Observations

The EXOS-C (Ohzora) satellite was launched on 14 February 1984 into a semi-polar orbit with an initial apogee and perigee of 865 and 354 km, a 74.6° orbital inclination, and a 96.1-min period. The plasma wave phenomena in the upper ionosphere were observed by the Planetary Plasma Sounder (PPS) Experiment. This experiment had two categories of observational function: Stimulated Plasma Wave Experiments (SPW) and Natural Plasma Wave Experiments (NPW). The observations of the natural plasma wave phenomena in the VLF range were made in the operational mode of NPW experiments in the VLF range (NPW-V). Electric field signals received by a dipole antenna with a 40-m tip-to-tip length were analyzed by a frequency-swept spectral analyzer on board the spacecraft. The analyzer swept the frequency from 0.5 to 20 kHz with a 125-ms time resolution and a 400-Hz frequency resolution. The dynamic range of the spectrum analyzer was 90 dB with a two-step gain control. The analyzed spectra were converted to digital data

(PCM data) and recorded on the onboard data-recorder. The time and frequency resolutions were sufficient to classify the VLF phenomena into whistlers, ELF and VLF hiss, and LHR emissions among others. A detailed description of the PPS system is given by Oya et al. (1985).

3 LHR band emissions

3.1 Spectral properties

The typical dynamic spectra of the VLF phenomena observed by EXOS-C (Ohzora) during the time when the spacecraft passed the Northern Hemisphere from middle to high latitude are illustrated in Fig. 1. The usual intense auroral hiss events were observed in the auroral region with distinct equatorward boundaries (Morioka and Oya, 1985). At lower latitudes, below the auroral region, emissions with a banded structure whose center frequency increased systematically as the magnetic latitude decreased were observed: from 5 to 20 kHz (upper panel of Fig. 1) and from 4 to 15 kHz (lower panel). These banded and continuous wave phenomena in the VLF range are typical LHR band emissions, as originally reported by the Alouette 1 satellite (Barrington and Belrose, 1963; Brice and Smith, 1965). The approximate frequency of the lower hybrid resonance is given by Brice and Smith (1965) as,

$$\left(\frac{1}{M_{\text{eff}}} \frac{m_e}{m_p} \right) \frac{1}{f_{\text{LHR}}^2} = \frac{1}{f_p^2} + \frac{1}{f_c^2}, \quad (1)$$

$$\frac{1}{M_{\text{eff}}} = \sum \frac{\alpha_i}{M_i}, \quad (2)$$

where f_{LHR} , f_p , f_c , m_e , and m_p are the lower hybrid resonance frequency, electron plasma frequency, electron gyro-frequency, electron mass and proton mass, respectively. α_i is the fractional amount of the i th ion, M_i is the atomic mass of the i th ion, and M_{eff} is the effective atomic mass. The systematic frequency variation in the LHR band emissions with respect to the magnetic latitude is caused by combined changes in plasma frequency, electron gyrofrequency, and ion composition along the satellite pass.

The expanded dynamic spectrum of the LHR band emission phenomena is shown in Fig. 2. One of the distinct spectral characteristics of the emission is the long-lasting banded structure with a typical bandwidth of about 2–3 kHz. Another notable characteristic of the phenomena is less burst-like features different in contrast to the auroral hiss, as can be seen in Figs. 1 and 2. This indicates that these emissions are generated continuously and steadily.

The typical frequency spectra of LHR band emissions are shown in Fig. 3 to illustrate the characteristic bandwidth and cut-off feature. The waves in the frequency range from 5 to 12 kHz in the figure are LHR band emissions, and the waves below 5 kHz are ionospheric ELF hiss. These spectra were obtained in the Southern Hemisphere at an altitude of approximately 650 km. The typical bandwidth of the LHR

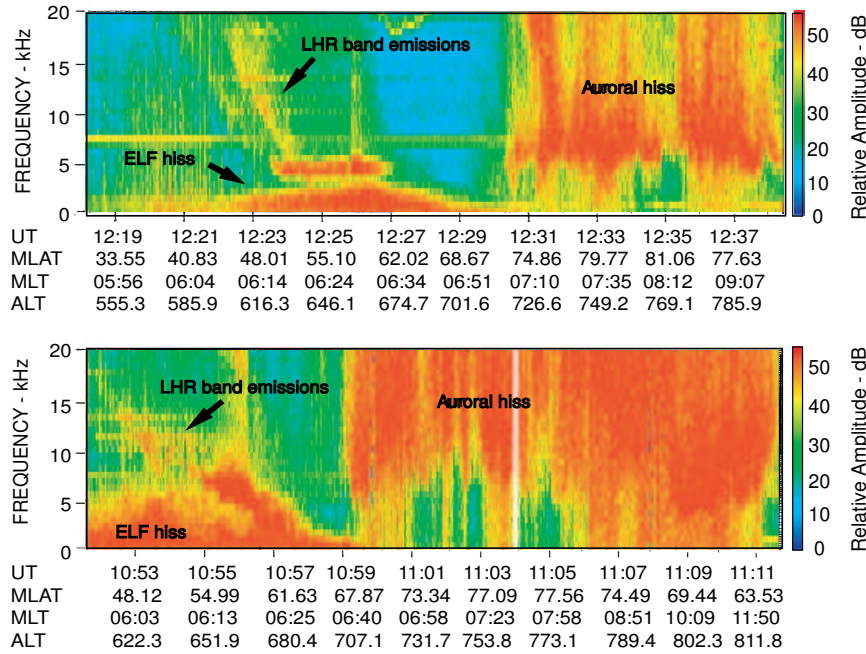


Fig. 1. Dynamic spectra of electric field observed in middle and auroral latitudes on two successive days on 17 and 18 October 1984.

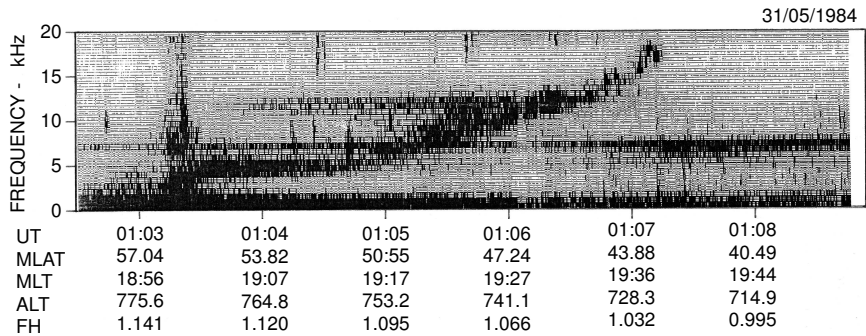


Fig. 2. Expanded dynamic spectrum of LHR band emissions observed on 31 May 1984.

emissions (half power bandwidth) was about 2–3 kHz. The ratio of the bandwidth to the center frequency ($\Delta f/f$) seems to be considerably large (30–50%) when we consider the local resonance of LHR waves. It is also noteworthy that the slope of the spectrum was fairly gradual at both sides of the spectral peak, with a spectral gradient of 10–15 dB/kHz. This feature suggests that the LHR band emissions are not the result of the cut-off effect of the descending whistler mode waves in the ionosphere.

3.2 Spatial distribution and relationship to magnetic activity

We selected typical 58 LHR band emissions during the period from 1 June to 7 November 1984, for the statistical analysis. The spatial distribution of 58 emissions is shown in Fig. 4. The satellite trajectories where the LHR band emissions were detected are plotted on the polar plot which is coordinated with an invariant latitude and magnetic local time.

The number of occurrences in the night-side region was low. This is partly because the satellite operation was restricted to a light power-load mode when the satellite was in the Earth’s eclipse, resulting in limited chances for NPW experiments. Thus, the local time distribution in Fig. 4 is inconclusive. However, it can be said that the LHR band emissions have no local time dependence, at least between the early morning and late evening. The latitudinal occurrence region of the emissions is distributed between 40° and 65° in invariant latitude, which correspond to $L=1.7\text{--}5.6$. The poleward boundary of the phenomena scarcely made contact with the average auroral oval (hatched area in the figure: Feldstein, 1963). This indicates that the LHR band emissions are not directly related to the auroral phenomena.

The relationship between the spatial distribution of LHR band emissions and the magnetic activity is illustrated in Fig. 5. The lower panel in the figure shows the K_p dependence on the invariant latitude of the emissions. The

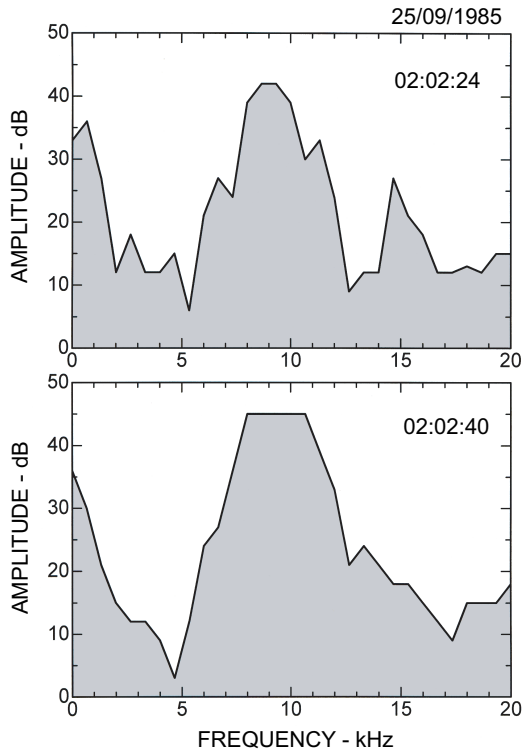


Fig. 3. Frequency spectra of LHR band emissions in the frequency range from 5 to 12 kHz and ELF hiss below 5 kHz detected near the plasmopause on 25 September 1985.

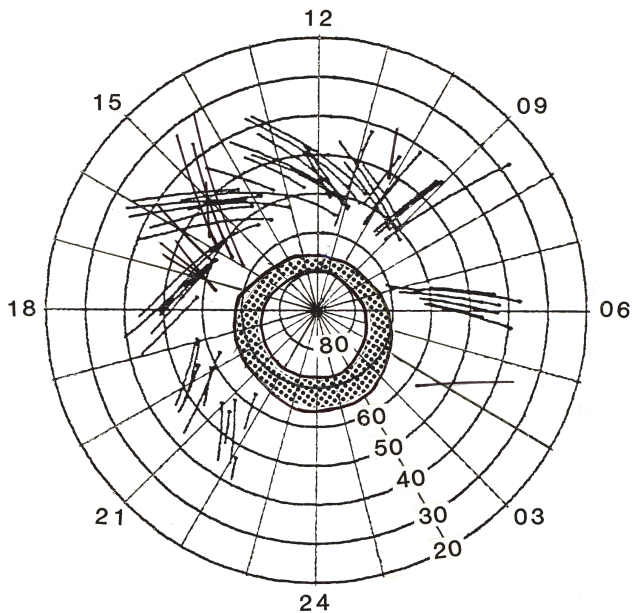


Fig. 4. Latitudinal and local-time distribution of LHR band emissions. The polar plot is coordinated with an invariant latitude and magnetic local time. The absence of LHR band emissions around midnight is due to our suspending satellite observations during that time. The hatched area shows the average auroral oval (Feldstein, 1963).

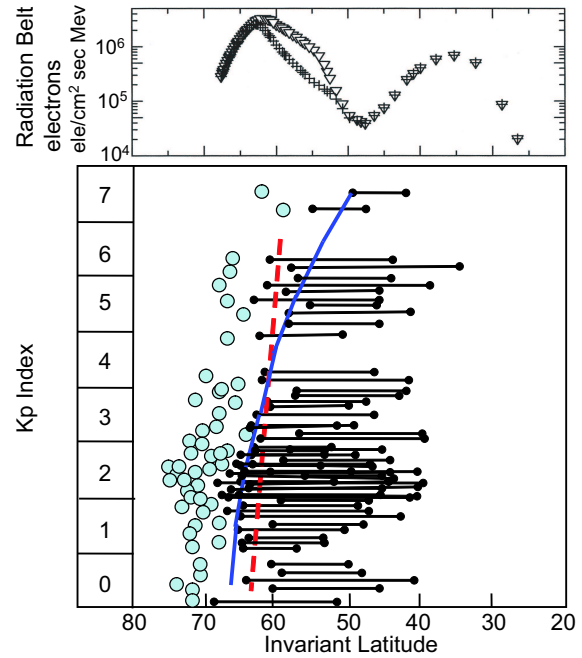


Fig. 5. Lower panel: K_p dependence of LHR band emissions with respect to invariant latitude. The horizontal solid lines indicate the latitudinal range of the emissions. The open circles show the lower latitude boundaries of the auroral hiss region. The blue line indicates the empirical plasmopause position. The red dotted-line indicates the average flux-peak position of the radiation belt electrons. Upper panel: Latitudinal distribution of the relativistic electrons of 1 MeV (AE-8 model). The triangles show the flux distribution during the solar maximum period and the crosses during the solar minimum period.

horizontal solid lines indicate the latitudinal range of the emissions, and the open circles show the lower latitude boundaries of the auroral hiss region, which could be a good indicator for the particle precipitation in the auroral region. The figure shows that the high-latitude boundaries of the LHR band emissions shift to lower latitudes as the magnetic activity increases. This tendency is almost parallel to the motion of the equatorward boundary of the auroral hiss emission (open circles in the figure). The oblique blue line in the lower panel shows the empirical plasmopause position (Carpenter and Anderson, 1992), where the instantaneous K_p is used instead of $K_{p\max}$ (maximum K_p during the preceding 24 h). The oblique red dotted-line in the lower panel indicates the average flux-peak position of the outer radiation belt electrons ($E > 300$ keV) with respect to the K_p index, which was statistically obtained from the data in 1984 using NOAA-6/MEPED (Raben et al., 1995) observations. These illustrations suggest that the poleward boundary of LHR band emissions is located near the plasmopause during low- K_p periods, and during disturbed periods, the boundary seems to follow the peak-flux position of the outer radiation belt.

The frequency range of the LHR band emission is statistically investigated as a function of the invariant latitude as shown in Fig. 6. The filled circles show the observed

lowest and highest frequencies of the emissions. Note that the straight lines do not show the frequency trace of each phenomenon but only the linear link between the lowest and highest frequencies, and that highest frequency of 20 kHz is not the natural upper limit of the emission but the instrumental limit of the receiver. Figure 6 shows that the average emission frequency in higher latitude is about 3 kHz, on average, and it increases up to 20 kHz or more as the invariant latitude decreases. The altitude distribution of the LHR band emissions was also investigated with respect to the invariant latitudes (Fig. 7a) and center frequencies of emissions (Fig. 7b). The straight lines in each panel show the intervals between the beginning and end of the phenomena. These statistical results show that observed LHR band emissions appear everywhere in the ionosphere, at least in the altitude range of the EXOS-C (Ohzora), without relation to both the invariant latitude and emission frequency, strongly suggesting that they are not always local resonance phenomena but propagating waves generated and trapped in the ionosphere.

3.3 Relationship with energetic particles and ionospheric heating

The LHR band emissions showed some relationships with electron heating phenomena in the topside ionosphere and energetic particles in the radiation belt. A typical example on 17 October 1984 is illustrated in Fig. 8. The LHR band emissions (top panel) were detected twice at middle latitudes in the morning and afternoon sector in the frequency range from 15 to 3 kHz and vice versa. The middle panel of Fig. 8 illustrates the simultaneous electron temperature detected by probes for the Temperature of Electron (TEL) (Oyama et al., 1985) on board the EXOS-C (Ohzora) satellite. We can see a clear electron-temperature enhancement of about 1000 K in the magnetic latitude range of 40°–60° in both the morning and afternoon sector. It should be noted that these electron temperature enhancement phenomena just coincide with the occurrence region of the LHR band emissions.

Low energy electrons with 16–300 eV and with 0.2–10 keV taken by the EXOS-C (Ohzora) (Mukai et al., 1985) showed good correlation with the auroral hiss, but they did not show any correspondence with the LHR band emissions (not shown). In looking at the quasi-trapped relativistic electron flux (0.19–3.2 MeV) data in the bottom panel (Nagata et al., 1985), it is suggested that the LHR band emissions appear in the lower latitude side of the outer belt. This implication of the relationship with the radiation belt can also be seen from the average distribution of trapped energetic electrons, as illustrated in Fig. 5. Triangles and crosses in the upper panel of Fig. 5 indicate the average fluxes of 1-MeV electrons during the solar maximum and minimum period, respectively, derived from the AE-8 model (Vette, 1991). From the comparison with the spatial distribution of the LHR band emissions (lower panel of Fig. 5), we can see that the emissions commonly lie in the slot region. The slot region has been considered to be the diffusive precipitation region of the relativistic electrons due to the pitch-angle scattering through the

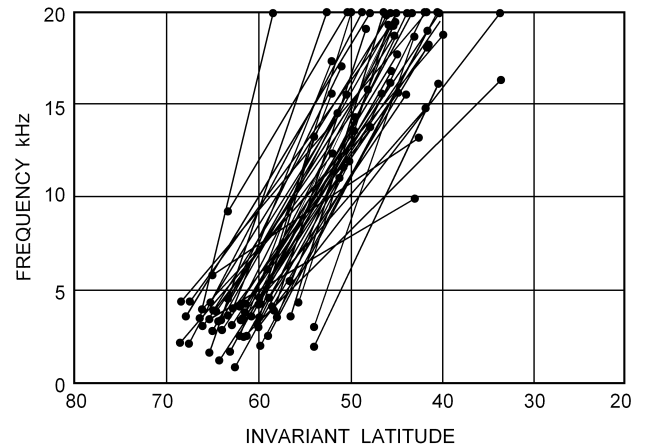


Fig. 6. Frequency band of the LHR band emissions with respect to invariant latitudes. The filled circles show the observed highest and lowest frequencies of the emissions. Note that the line connecting two circles is not the frequency trace of the phenomena.

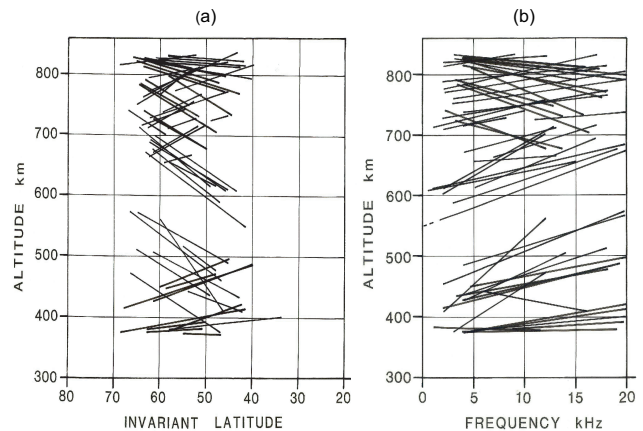


Fig. 7. Altitude distribution of the LHR band emissions with respect to invariant latitudes (a) and frequencies (b). Straight lines in each panel show intervals between the beginning and end of phenomena.

wave particle interaction with plasmaspheric hiss (Lyons et al., 1972; Lyons and Thorne, 1973; Abel and Thorne, 1998).

3.4 Correlation with ionospheric ELF hiss

The EXOS-C (Ohzora) observations showed that the LHR band emissions have a close relationship with the ionospheric ELF hiss. As can be seen in the dynamic spectra of Fig. 1, ionospheric ELF waves below approximately 3 kHz were simultaneously observed with LHR band emissions, while the auroral hiss shows little correlation with the ELF waves. The simultaneous occurrence of the ionospheric hiss with the LHR band emissions is also illustrated in Fig. 3, where the ionospheric ELF waves have larger amplitude as the frequency decreases. The correlated occurrence between LHR band emissions and ELF hiss was statistically analyzed from the 1984 observation data. LHR band emission events

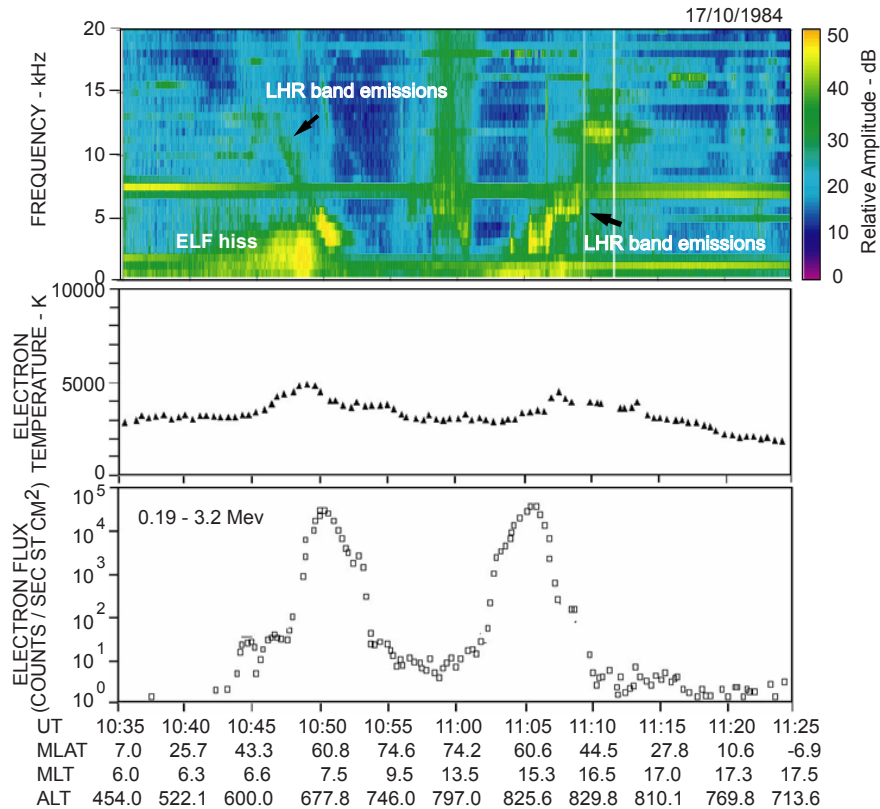


Fig. 8. Relationship among the LHR band emissions, the ionospheric electron temperature, and the energetic particle phenomena on 17 October 1984. Top panel: Dynamic spectrum of the VLF waves. LHR band emissions were detected in the middle latitude between about 43° and 60°. Second panel: electron temperature. Third panel: relativistic electron flux (0.19 to 3.2 MeV).

and ionospheric ELF hiss events were separately picked up and listed. Then the rates of the coincident and exclusive occurrence of these events were investigated. The results showed that the probability of both waves appearing simultaneously was 79.7%. However, the probability of LHR emissions without ELF phenomena was 9.4% and that of ELF emissions without LHR phenomena was 10.9%. This means that the occurrence of both events is strongly related, although it is not certain which one is primary and which one is secondary.

4 Discussion

4.1 Ducted propagation

As mentioned in the Introduction, three categories of occurrence mechanisms have been considered for interpreting the LHR band emission phenomena: (1) cut-off phenomena of the waves descending from the topside ionosphere or the magnetosphere, (2) a local resonant emission generated in the ionosphere, or (3) trapped waves in the ionospheric duct. The first possibility (cut-off phenomena) was claimed by Storey and Cerisier (1968). They showed that non-ducted whistler mode waves have a large energy density at the altitude where the waves are reflected in the ionosphere near

the LHR frequency because the waves near that frequency stay in a certain altitude range longer during the reflection process. However, the LHR waves observed at mid-latitude by EXOS-C (Ohzora) did not show a cut-off signature but a banded nature with a gradual slope of the spectrum at both sides of its spectral peak as illustrated in Fig. 3. This indicates that the cut-off effect at the LHR frequency is not essential for the present LHR wave phenomena.

The second likely source of mid-latitude LHR is the in-situ waves generated near the LHR frequency (Barrington et al., 1965; Taylor et al., 1969; Horita and Watanabe, 1969). Laaspere and Taylor (1970) reported that the frequency of the LHR waves corresponds to local ion composition. However, they also presented that the observed LHR frequency is not always determined in the immediate vicinity of the spacecraft. This observational discrepancy can be understood from the present investigation that the detected LHR emissions are not only generated waves in the vicinity of the satellite but also trapped and propagating ones in the ionosphere, because the observed emissions have a relatively wide bandwidth compared with the center frequency and they distribute in a wide altitude range in the ionosphere.

The third mechanism to explain mid-latitude LHR band emissions is the propagation in the duct formed horizontally in the upper ionosphere. Kimura (1966) first showed that the

horizontal VLF duct can be formed above the ionospheric F layer associated with the lower hybrid resonance. Smith et al. (1966) suggested that the LHR band waves are the result of the duct propagation of the auroral hiss. To explain the bandwidth of the VLF banded hiss, Gross (1970) calculated the duct properties under the conditions of a diffusive equilibrium ionosphere. The result showed that the VLF ducts can be formed and that the possible bandwidth is of the order of 2.5 to 3 kHz. Here, we examined the vertical profile of the LHR frequency in the ionosphere using the International Reference Ionosphere model (IRI2001; Bilitza, 2001) referring to the 31 May 1984 data (Fig. 2). Figure 9 shows calculated altitude profiles of the LHR frequency (solid line) and M_{eff} (solid broken line) at the time of 01:05:30 UT in Fig. 2, where the magnetic latitude and magnetic local time are 49° and 19.2 h, respectively. The result demonstrates well the ionospheric trapping of the LHR waves in the frequency range between the minimum LHR frequency and the smaller of the two maximum frequencies, as proven by Smith et al. (1966) and Gross (1970). This trapping corresponds to the frequency range from 5.8 to 7.5 kHz in the altitude range from 250–840 km, as indicated by the hatched area in Fig. 9. These calculated features roughly agree with the observed frequency range and its bandwidth in Fig. 2 and with the observed altitude range of the LHR by the EXOS-C (Ohzora), as seen in Fig. 7. Thus, the horizontally-formed LHR duct is most reasonable to interpret the fundamental features of the mid-latitude LHR band emissions as originally discussed by Smith et al. (1966) and Gross (1970). Their speculation that the origin of the ducted LHR is the auroral hiss is, however, not evident, as can clearly be seen in Figs. 1, 4, and 5. The LHR phenomena at mid-latitude are not connected to the auroral hiss. At the latitude of the ionospheric trough region, the LHR duct disappears due to specific changes in electron density and ion composition, as shown by the thin broken line in Fig. 9, where ionospheric conditions are obtained from IRI2001 referring to the spacecraft location at 01:02:30 UT (magnetic latitude of 58°) in Fig. 2. Thus, the mid-latitude LHR band emissions are separated from the auroral region. Based on these considerations, we conclude that the mid-latitude LHR band phenomena should originate in the topside ionosphere and become trapped in the ionospheric LHR duct.

4.2 Relationship to energetic particles and ionospheric ELF hiss

The LHR banded emissions have no relationship with lower energy particles, at least in the energy range of 200 eV to 16 keV, as observed by the Energy Spectrum of Particles (ESP) on board the EXOS-C (Ohzora). However, the LHR phenomena have been found to occur around the region where the relativistic electrons show a slot between the inner and outer radiation belts. Quantitative studies have shown that the resonant interaction with whistler mode waves causes a pitch-angle diffusion of the radiation belt electrons (Kennel and Petschek, 1966; Lyons et al., 1972). It has also

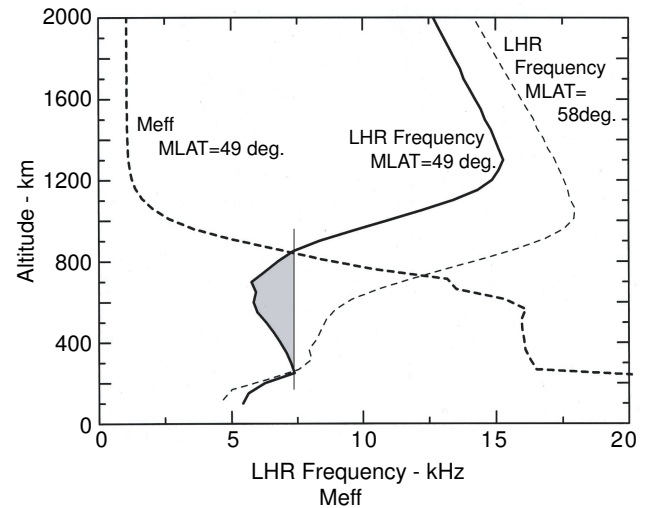


Fig. 9. LHR frequency and M_{eff} distribution with respect to altitude calculated from IRI2001 model. The solid and solid broken lines are LHR frequency and M_{eff} profiles, respectively, corresponding to the geographical and geomagnetic coordination at 01:05:30 UT in Fig. 2. The hatched portion on the LHR frequency profile shows the ionospheric LHR duct. The thin broken line indicates the LHR frequency profile at around the ionospheric trough region corresponding to 01:02:30 UT in Fig. 2.

been widely accepted that plasmaspheric ELF hiss generated through cyclotron resonant instability (Thorne et al., 1973) should result in the formation of the slot region due to scattering of radiation belt electrons into the ionosphere (Lyons et al., 1972; Lyons and Thorne, 1973). On the other hand, electromagnetic ion cyclotron waves (EMIC) can also precipitate relativistic electrons through the pitch-angle scattering (Thorne and Kennel, 1971; Lyons and Thorne, 1972; Thorne, 1974; Albert, 2003). Summers and Thorne (2003) calculated the detailed pitch-angle diffusion rate due to EMIC waves under the magnetically disturbed condition and showed the efficient precipitation of the relativistic electrons. Thus, there remains a possible discussion that EMIC waves might cause the slot of the radiation belt, although it is not certain that the waves are detectable in the deep inner-magnetosphere around the slot region.

It has been suggested that ELF hiss in the ionosphere is the penetrated component of the plasmaspheric hiss. Studies by polar-orbiting ionospheric satellites (e.g. Thorne et al., 1974; Smith et al., 1974; Ondoh et al., 1983) showed that characteristics of the ionospheric ELF hiss is very similar to those of the plasmaspheric ELF hiss, and thus the ionospheric ELF hiss is considered to be generated in the plasmasphere. Muzzio and Angerami (1972) and Ondoh et al. (1983) showed, by means of the ray-tracing method, that whistler mode waves with a large wave-normal angle in the plasmaspheric equatorial region can penetrate into the ionosphere, indicating that the ionospheric ELF hiss is the penetrated component of the plasmaspheric ELF hiss. Thus, the existence of ionospheric ELF hiss may indirectly

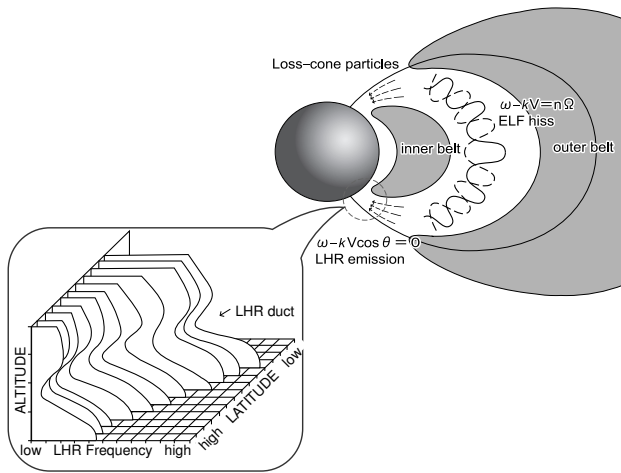


Fig. 10. Schematic illustration of the hypothesis responsible for LHR band emission generation.

manifest the precipitation of energetic electrons scattered by plasmaspheric hiss, and the strong correlation between LHR emissions and the ionospheric ELF hiss may suggest the excitation of LHR waves by precipitated energetic electrons.

Recently, Meredith et al. (2004) reported that the plasmaspheric hiss amplitudes depend on substorm activity, and suggested that the enhanced hiss during the substorm activity will cause the increase of pitch-angle scattering and play a significant role in radiation belt electron dynamics. Their result seems to be rather consistent with the present analysis in Fig. 1. The upper spectrogram in the figure was observed during the medium intensity substorm of $AE^*=152$ nT, and bottom spectrogram was observed during the intense substorm of $AE^*=794$ nT. Here, AE^* is the maximum value of the AE index in the previous 3 h defined by Meredith et al. (2004). We can see that ionospheric ELF hiss and LHR band emissions showed the more intense amplitude and wider frequency band during the intense substorm (bottom panel) compared with the medium intensity substorm (upper panel). This feature can be understood that the intensification of ionospheric ELF hiss will correspond to the propagation of the enhanced plasmaspheric hiss and the intense LHR emission will be the result of the reinforced energetic electron precipitation.

The coincidence between the mid-latitude LHR band emissions and the enhanced electron-temperature structure in the topside ionosphere was found in this study. The mid-latitude ionospheric trough is known to show the enhanced electron temperature due to heat conduction from the plasmasphere near the plasmopause (e.g. Rees and Roble, 1975; Burke et al., 1979; Kozyra et al., 1986). However, the enhanced structure of electron temperature which coincides with the latitudinal range of the LHR band emissions, as detected in this study, is found to be different from the mid-latitude ionospheric trough, because the present phenomena occur inside the plasmasphere, at least during magnetically quiet periods, as seen in Fig. 5, and the latitudinal

range of the interested phenomena is wider than that of the mid-latitude ionospheric trough (e.g. Watanabe et al., 1989; Werner and Pröls, 1997). One of the possible heat sources for the present phenomena may be the LHR wave itself. However, the energy density of the wave seems too low to heat up the plasma in the topside ionosphere. Thus, the heating process of the present temperature enhancement of ionospheric electrons is quite uncertain at this time.

4.3 Generation of mid-latitude LHR band emissions

Based on the observed results, we herein discuss the generation of LHR band emissions. In the plasmasphere, the drizzly precipitation due to the pitch-angle scattering of energetic electrons takes place through a cyclotron resonant interaction with the plasmaspheric hiss. These loss-cone electrons into the ionosphere may become the free energy source of the LHR emissions. For the fundamental wave-particle interaction relating to the LHR band emissions, the Landau interaction,

$$\omega - kV \cos \theta = 0, \quad (3)$$

is most likely because the resonance condition can be satisfied for a wide range of particle energy at the LHR branch, where ω , k , V , and θ are the wave frequency, the wave number, the particle velocity, and a wave normal angle, respectively. LHR waves that have a large wave normal angle with respect to the magnetic field can interact with the precipitating energetic electrons with a relatively small value of $V \cos \theta$. After the LHR waves are generated in the ionosphere, they can become trapped in the duct in the upper ionosphere, as shown by Smith et al. (1966) and Gross (1970) and in Fig. 9. Figure 10 illustrates the synopsis of the present scenario responsible for the generation of the LHR band emissions.

5 Summary and conclusions

We derived some occurrence characteristics of LHR band emissions in the upper ionosphere using VLF spectral observations with the EXOS-C (Ohzora) satellite:

1. The LHR band emissions observed at mid-latitude indicated clear banded-spectra without burst-like and cut-off features. The emission frequency changed roughly from 3 to 20 kHz as the spacecraft moved from subauroral to lower latitude. The bandwidth of the emissions is relatively wide with $\Delta f/f=0.3-0.5$.
2. The latitudinal range of the LHR band emissions was from 40° to 65° corresponding to $L=1.7-5.6$. The poleward boundary of the phenomena was separated from the auroral oval and seems to correspond with the plasmopause during magnetically quiet periods.
3. The spatial distribution showed the relationship with the magnetic activity. The high latitude boundary of the

emissions moved toward lower latitudes as the K_p index increased. This latitudinal motion with the magnetic activity seems to correspond with that of both the plasma-pause position and peak-flux position of the outer radiation belt.

4. The LHR band emissions were detected in the whole altitude range of (f the EXOS-C (Ohzora) satellite – does not make sense) from 380 to 860 km without a dependence on frequency and invariant latitude, indicating that the emissions are not always in-situ resonance waves but trapped waves in the ionospheric duct.
5. The emissions showed no local time dependence at least between the early morning and late evening. The occurrence at night was inconclusive due to a lack of observational data.
6. Ionospheric ELF waves and the LHR band emissions showed a good correspondence; they have a simultaneous occurrence probability of about 80%.
7. The observations showed that the LHR band emissions are commonly detected in the slot region of the relativistic electrons.
8. The observations also revealed the enhanced electron-temperature structure which coincides with the latitudinal range of the LHR band emission.

From these observed characteristics, we suggested that the LHR band emissions are waves trapped in the horizontally-formed LHR duct in the upper ionosphere. A hypothesis for the generation of the LHR band emissions in the ionosphere is proposed: precipitating radiation belt electrons scattered through an interaction with the plasmaspheric ELF hiss excite the LHR waves near the LHR frequency through Landau type wave-particle interactions. Then, the LHR waves generated in the topside ionosphere are trapped in the LHR duct.

Acknowledgements. We are grateful to T. Mukai for his support and for providing data from the Energy Spectrum of Particles (EPS) onboard the EXOS-C (Ohzora) satellite. We used the radiation belt data from AE-8/AP-8 Radiation Belt Models provided by the NSSDC. The IRI2001 data was also provided from NSSDC. The data from the NOAA satellite was obtained from the NOAA/POES data file through the National Geophysical Data Center (NGDC) via WDC-C2 for Aurora, the National Institute of Polar Research, Japan.

Topical Editor M. Lester thanks two referees for their help in evaluating this paper.

References

- Abel, B. and Thorne, R. M.: Electron scattering loss in Earth's inner magnetosphere: 1. Dominant physical processes, *J. Geophys. Res.*, 103, 2385–2396, 1998.
- Albert, J. M.: Evaluation of quasi-linear diffusion coefficients for EMIC waves in a multispecies plasma, *J. Geophys. Res.*, 108(A6), 1249, doi:10.1029/2002JA009792, 2003.
- Anderson, R. R. and Gurnett, D. A.: Observations of the lower hybrid resonance phenomena on the Injun 5 satellite, paper presented at URSI Spring Meeting, Washington, D. C., April, 1969.
- Barrington, R. E. and Belrose, J. S.: Preliminary results from the very-low-frequency receiver aboard Canada's Alouette satellite, *Nature* 198, 18 May, 651–656, 1963.
- Barrington, R. E., Belrose, J. S., and Keeley, D. A.: Very-low-frequency noise observed by the Alouette 1 satellite, *J. Geophys. Res.*, 68, 6539–6541, 1963.
- Barrington, R. E., Belrose, J. S., and Nelms, G. N.: Ion composition and temperatures at 1000 km as deduced from simultaneous observations of a VLF plasma resonance and top side sounding data from Alouette 1 satellite, *J. Geophys. Res.*, 70, 1647–1664, 1965.
- Bell, T. F., Inan, U. S., Lauben, D., Sonwalkar, V. S., Helliwell, R. A., Sobolev, Y. P., and Chmyrev, V. M.: DE-1 and COSMOS 1809 observations of lower hybrid wave excited by VLF whistler mode waves, *Geophys. Res. Lett.*, 21, 653–656, 1994.
- Bilitza, D.: International Reference Ionosphere 2000, *Radio Sci.*, 36, 261–275, 2001.
- Boskova, L., Jiříček, F., and Triska, P.: Latitude variation of the LHR frequency in the outer ionosphere as an indicator of the degree of magnetospheric perturbation, *Studia Geophysica et Geodaetica*, 27, 298–304, 1983.
- Boskova, J., Jiříček, F., Smilauer, J., Triska, P., Lundin, B. V., Shklyar, D. R., and Titova, E. E.: LHR whistlers and LHR spherics in the outer ionosphere, *J. Atmos. Terr. Phys.*, 54, 1321–1328, 1992.
- Brice, N. and Smith, R. L.: Recordings from satellite Alouette 1: A very-low-frequency plasma resonance, *Nature* 203, Aug. 29, 926–927, 1964.
- Brice, N. and Smith, R. L.: Lower hybrid resonance emissions. *J. Geophys. Res.*, 70, 71–80, 1965.
- Burke, W. J., Braum, H. J., Munch, J. W., and Sagalyn, R. C.: Observations concerning the relationship between the quiet-time ring current and electron temperature at trough latitudes, *Planet. Space Sci.*, 27, 1175–1185, 1979.
- Burtis, W. J.: Electron concentration calculated from the lower hybrid resonance noise band observed by Ogo 3, *J. Geophys. Res.*, 78, 5515–5523, 1973.
- Carpenter, D. L. and Anderson, R. R.: An ISEE/whistler model of equatorial electron density in the magnetosphere, *J. Geophys. Res.*, 97, 1097–1108, 1992.
- Chum, J., Jiříček, F., and Shklyar, D.: Lhr associated oblique noise bands, paper presented at EGS XXXVII General Assembly, Nice, 21–26, 2002.
- Feldstein, Y.: Some problems concerning the morphology of auroras and magnetic disturbances at high latitudes, *Geomag. Aeron.*, 3, 183–192, 1963.
- Gross, S. H.: VLF duct associated with the lower-hybrid-resonance frequency ins multi-ion upper ionosphere, *J. Geophys. Res.*, 75, 4235–4247, 1970.
- Horita, R. E. and Watanabe, T.: Electrostatic waves in the ionosphere excited around the lower hybrid resonance frequency, *Planet. Space Sci.*, 17, 61–74, 1969.
- Jiříček, F., Shklyar, D. R., and Tiska, P.: LHR effects in nonducted whistler propagation – new observations and numerical modelling, *Ann. Geophys.* 19, 147–157, 2001.
- Kennel, C. F. and Petschek, H. E.: Limit on stably trapped particle fluxes, *J. Geophys. Res.*, 70, 1–28, 1966.
- Kimura, I.: Effects of ions on whistler-mode ray tracing, *Radio Sci.*, 1, 269–283, 1966.

- Kozyra, J. U., Brace, L. H., Cravens, T. E., and Nagy, A. F.: A statistical study of the subauroral electron temperature enhancement using Dynamics Explorer 2 Langmuir probe observations, *J. Geophys. Res.*, 91, 11 270–11 280, 1986.
- Laaspere, T., Morgan, M. G., and Johnson, W. C.: Observations of lower hybrid resonance phenomena on the OGO 2 spacecraft, *J. Geophys. Res.*, 74, 141–152, 1969.
- Laaspere, T. and Taylor, H. A.: Comparison of certain VLF noise phenomena with the lower hybrid resonance frequency calculated from simultaneous ion composition measurements, *J. Geophys. Res.*, 75, 97–106, 1970.
- Laaspere, T., Johnson, W. C., and Semperebon, L. C.: Observations of auroral hiss, LHR noise, and other phenomena in the frequency range 20 Hz–540 kHz on OGO 6, *J. Geophys. Res.*, 76, 4477–4493, 1971.
- Lyons, R. L., Thorne, R. M., and Kennel, C. F.: Pitch angle diffusion of radiation belt electrons within the plasmasphere, *J. Geophys. Res.*, 77, 3455–3474, 1972.
- Lyons, R. L. and R. M. Thorne, Particle pitch angle diffusion of radiation belt particles by ion cyclotron waves, *J. Geophys. Res.*, 77, 5608–5616, 1972.
- Lyons, R. L. and Thorne, R. M.: Equilibrium structure of radiation belt electrons, *J. Geophys. Res.*, 78, 2142–2149, 1973.
- McBride, J. B. and Pytte, A.: Influence of Coulomb collisions on electrostatic waves in the ionosphere, *Planet. Space Sci.* 18, 155–158, 1970.
- McEwen D. J. and Barrington, R. E.: Some characteristics of the lower hybrid resonance noise bands observed by the Alouette satellite, *Can. J. Phys.*, 45, 13–20, 1967.
- Meredith, N. P., Horne, R. B., Thorne, R. M., Summers, D., and Anderson, R. R.: Substorm dependence of plasmaspheric hiss, *J. Geophys. Res.*, 109, A06209, doi:10.1029/2004JA010387, 2004.
- Mikhailov, Y. M., Kapustina, O. V., Ershova, V. A., Roste, O. Z., Shultchishin, Y. A., Kochnev, V. A., and Shmilauer, Y.: Definition of the lower hybrid frequency by active wave methods on the INTERCOSMOS-24 satellite and comparison of these data with mass-spectrometric measurements, *Adv. Space Res.*, 15, 147–150, 1995.
- Morioka, A. and Oya, H.: Emissions of plasma waves from VLF to LF ranges in the magnetic polar regions — New evidences obtained from the Ohzora (EXOS-C) satellite, *J. Geomag. Geoelectr.*, 37, 263–284, 1985.
- Mukai, T., Kubo, H., Itoh, T., Kaya, N., and Matsumoto, H.: Initial observation of low-energy charged particles by satellite Ohzora (EXOS-C), *J. Geomag. Geoelectr.* 37, 365–387, 1985.
- Muzzio, J. L. R. and Angerami, J.: Ogo 4 observations of extremely low frequency hiss, *J. Geophys. Res.*, 77, 1157–1173, 1972.
- Nagata, K., Kohno, T., Murakami, H., Nakamoto, A., and Hasebe, N.: OHZORA high energy particle observations, *J. Geomag. Geoelectr.*, 37, 329–345, 1985.
- Nishino, M. and Tanaka, Y.: Observations of auroral LHR noise by the sounding rocket S-310JA-6, *Planet. Space Sci.* 35, 127–137, 1987.
- Ondoh, T. and Murakami, T.: Mid-latitude VLF emissions observed in the topside ionosphere, *Rep. Ionos. Space Res. Japan*, 29, 23–30, 1975.
- Ondoh, T., Nakamura, Y., Watanabe, S., Aikyo, K., and Murakami, T.: Plasmaspheric hiss observed in the topside ionosphere at mid- and low-latitudes, *Planet. Space Sci.*, 31, 411–423, 1983.
- Oya, H., Morioka, A., and Obata, T.: Leaked AKR and terrestrial hectometric radiations discovered by the plasma wave and planetary plasma sounder experiments on board the EXOS-C (Ohzora) satellite – Instrumentation and observation results of plasma wave phenomena, *J. Geomag. Geoelectr.*, 37, 237–262, 1985.
- Oyama, K.-I., Hirao, K., and Yasuhara, F.: Electron temperature probe on board Japan's 9th scientific satellite OHZORA, *J. Geomag. Geoelectr.*, 37, 413–430, 1985.
- Raben, V. J., Evans, D. E., Sauer, H. H., Sahn, S. R., and Huynh, M.: TIROS/NOAA satellite space environment monitor data archive documentation: 1995 update, NOAA Tech. Memo. ERL SEL-86, 1995.
- Rees, M. H. and Roble, R. G.: Observations and theory of the formation of stable auroral red arcs, *Rev. Geophys.*, 13, 201–242, 1975.
- Smith E. J., Frandsen, S. M. A., Tsurutani, B. T., Thorne, R. M., and Chan, K. W.: Plasmaspheric hiss intensity variations during magnetic storms, *J. Geophys. Res.*, 79, 2507–2510, 1974.
- Smith, R. L., Kimura, I., Vigneron, J., and Katsufakis, J.: Lower hybrid resonance noise and a new ionospheric duct, *J. Geophys. Res.*, 71, 1925–1927, 1966.
- Storey, O. and Cerisier, J. C.: Une interpretation des bandes de bruit au voisinage de la frequence hybride basse observees au moyen de satellites artificiels, *Comt. Rend.*, Ser. B, 266, 525, 1968.
- Summers, D. and Thorne, R. M.: Relativistic electron pitch angle scattering by electromagnetic ion cyclotron waves during geomagnetic storms, *J. Geophys. Res.*, 108(A4), 1143, doi:10.1029/2002JA009489, 2003.
- Taylor, H. A. Jr., Brinton, H. C., Carpenter, D. L., Bonner, F. M., and Heyborne, R. L.: Ion depletion in the high latitude exosphere; simultaneous OGO 2 observations of the light ion trough and the VLF cutoff, *J. Geophys. Res.*, 74, 3517–3528, 1969.
- Thorne, R. M.: A possible cause of dayside relativistic electron precipitation events, *J. Atmos. Terr. Phys.*, 36, 635–645, 1974.
- Thorne, R. M., Smith, E. J., Burton, R. B., and Holtzer, R. E.: Plasmaspheric hiss, *J. Geophys. Res.*, 78, 1581–1596, 1973.
- Thorne, R. M. and Kennel, C. F.: Relativistic electron precipitation during magnetic storm main phase, *J. Geophys. Res.*, 76, 4446–4453, 1974.
- Thorne R. M., Smith, E. J., Fiske, J., and Holzer, R. E.: Intensity variation of ELF hiss and chorus during isolated substorms, *Geophys. Res. Lett.*, 1, 193–196, 1974.
- Tjulin, A., Eriksson, A. I., and André, M.: Lower hybrid cavities in the inner magnetosphere, *Geophys. Res. Lett.*, 30, 1364, doi:10.1029/2003GL016915, 2003.
- Vette, J.: The AE-8 trapped electron model environment, National Space Science Data Center, Rep. 91-24, Green Belt, Md, 1991.
- Watanabe, S., Oyama, K.-I., and Abe, T.: Electron temperature structure around mid latitude ionospheric trough, *Planet. Space Sci.*, 37, 1453–1460, 1989.
- Werner, S. and Pröls, G. W.: The position of the ionospheric trough as a function of local time and magnetic activity, *Adv. Space Res.*, 20, 1717–1722, 1997.